PERGAMON

International Journal of Solids and Structures 38 (2001) 8907–8920

INTERNATIONAL JOURNAL OF SOLIDS and STRUCTURES

www.elsevier.com/locate/ijsolstr

An inverse method for determining material properties of a multi-layer medium by boundary element method

Wenqing Wang *, Haruo Ishikawa, Hironobu Yuki

Department of Mechanical Engineering and Intelligent Systems, The University of Electro-Communications, 1-5-1 Chofugaoka, Chofu-shi, 182-8585 Tokyo, Japan

Received 15 March 2000

Abstract

An optimization system, which combines a particular boundary element method and a modified Levenberg–Marqardt method, and which can be used to determine material properties of a multi-layer medium from the specified or observed displacements, is presented in this paper. © 2001 Elsevier Science Ltd. All rights reserved.

Keywords: Inverse problem; Multi-layer medium; Boundary element method; Optimization system; Hankel's transform

1. Introduction

In recent years, more and more thin layered structures, such as thin films in electronic devices, sensors and actuators in smart materials and coatings on machine components for wear resistance, corrosion inhibition, or friction reduction, are being utilized in many industries. In order to analyze the mechanical behaviors of such layered structures, the mechanical properties of such layered materials had to be investigated at first. That is why the depth-sensing indentation test has been widely used in present days. With the indentation tests, one of the procedures for determining the material properties will finally come down to the analytical or numerical modeling of an elastic contact problem of a homogeneous body and a multi-layered structure. The pioneer work of the modeling was done by Loubet et al. (1984) using the elastic solution to a problem of a rigid cylindrical punch indenting a homogeneous half space. After that, Doerner and Nix (1986) extended the idea of Loubet et al. to the case of indentation of thin films deposited on substrates, King (1987) performed an integral equation analysis and modified the formula proposed by Doerner and Nix to fit his numerical results, and Shield and Body (1989) presented a solution of the problem of an axisymmetrical rigid punch indenting a layered half space by using integral transforms. Another integral equation approach for the axisymmetrical contact problem involving an elastic layer either in frictionless contact or perfectly bonded to an elastic half space was presented by Yu et al. (1990).

* Corresponding author.

E-mail addresses: wwang@mce.uec.ac.jp, wang_wenqing@hotmail.com (W. Wang), ishikawa@mce.uec.ac.jp (H. Ishikawa), yuki@mce.uec.ac.jp (H. Yuki).

0020-7683/01/$ - see front matter
PII: S0020-7683(01)00061-0

Subsequently, an important work was done by Gao et al. (1992), which employed a moduli-perturbation method to construct a closed-form, first-order-accurate solution for the contact compliance of a nonhomogeneous medium with a layered or continuously varying moduli in the depthwise direction, and the method presented in this work is now being used to determine the mechanical properties from micro- and nano-indentation data (Swain, 1998; Menick et al., 1999; Tsui and Pharr, 1999). Apart from the above-mentioned semi-analytical studies, the finite element method were also used to indentation test modeling by Bhattacharya and Nix (1988) and Laursen and Simo (1992).

Since the inverse problems may be designed to determine the unknowns from the specified or the measured system response, the present work treats the determination of the material properties of a multi-layered medium with the axisymmetrical punch indenting test results as an inverse problem, and then, presents a boundary element approach for this inverse problem. Compared with direct problems, the inverse problems perform essentially in backward way. We have the output, but we want the input. Our goal is to match the numerical results and measured results or specified data as closely as possible by numerical simulation, and then to estimate the some characteristics of specified materials. For inverse problems, the well posedness, which includes existence, uniqueness and continuity, is more important. The uniqueness of the solution is of greatly concerned because the actual physical conditions can be represented by only one solution. We can obtain more reasonable results from a well-posed inverse problem than an ill-posed problem. If suitable constraints are chosen for an ill-posed inverse problem, the well posedness of the problem will be satisfied (Trujillo, 1997). Generally, the process to solve the inverse problems may combine an optimization scheme, where a cost function determined by somehow comparing the known output and the numerical results must be minimized. Therefore, the process for solving this inverse problem comes down to finding the best method for minimizing the cost function. The minimizing schemes, such as the least squares methods, regularization and so on, are frequently used in optimization process of the inverse problems.

The boundary element method is a powerful alternative numerical technique other than the finite element method (Becker, 1992). Up to now, some literature on the solution of inverse problems has been devoted to the usage of boundary element methods as a numerical tool to solve the inverse problems. Chiang and Dulikravich (1986) used a boundary element method to calculate the size and the location of circular coolant flow passages in a composite turbine blade from prescribed temperature and heat flux distribution on the boundary. Zabaras et al. (1989) calculated surface traction from measurements of internal displacements using boundary element method with an assumption of elastic material behavior. Tanaka and Yamagiwa (1989) solved for the shape of internal defect using eigenfrequency data by boundary element method.

The present work addresses a problem for determining material properties of a multi-layer medium from the specified or observed displacements. The problems is physical and geometric axisymmetric. To avoid element discretization at layer interfaces and re-mesh during the optimization procedure, a particular boundary integral equation for the multi-layered media, which was presented by Wang and Ishikawa (1999, 2000), is incorporated in the optimization process. A modified Levenberg–Marqardt method (Ravi and Jennings, 1990) is adopted to match the displacements of a designed model and the results of the particular boundary element.

2. Problem definition and the boundary element approach

Herewith, we consider a large multi-layered media, the upper surface of which is pushed by a small homogeneous axisymmetric body, shaped as circular cylinder, cone, sphere etc. The prototype of this problem may be found in micro-indentations and geo-technique engineering. It is assumed that the multi-layered media may have N different layers, and the material in each layer is homogeneous, isotropic and

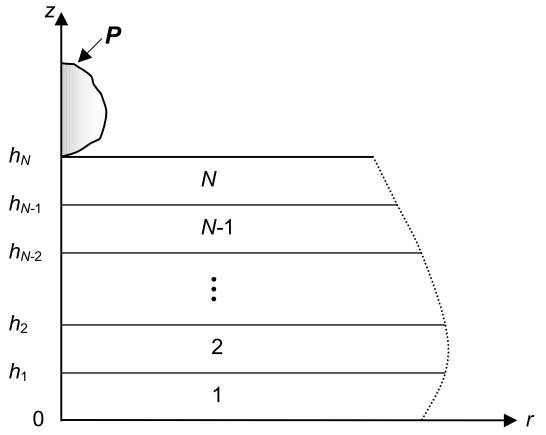

Fig. 1. Model for analysis.

linear elastic. It is also assumed that the prescribed loads are axisymmetric too. The model of this problem is depicted in Fig. 1, where h_i $(i = 1, 2, \ldots, N)$ is the height of interface or top surface.

Obviously, the mechanical behavior of each layer is governed by Navier's equation and constitutive law in cylindrical coordinate, and the mechanical behavior of the indentation can be described as a contact problem. Here, the boundary element method is used to analyze the contact problem.

If ordinary boundary element method, which uses Kelvin's solution as the fundamental solution, is adopted to analyze this contact problem of multi-layered medium indented by a punch, elements discretization must be taken to each interface between any two adjacent layers in multi-layered zone. That will increase the number of the freedom of system equations rapidly, especially for the case of the layer thickness varying in a large scale. Moreover, element re-mesh should be usually needed during the optimization procedure if the ordinary boundary element method was used. Therefore, the advantage of using boundary element methods may be decreased. In the present study, a new boundary element method is employed to simulate the contact behaviors. In the procedure of boundary element calculation, two different boundary integral equations are adopted for homogeneous region, which is occupied by indenter, and multi-layered region, respectively. For the former region, Kelvin's solution for elasto-static axisymmetric problem acts as the fundamental solution. For the latter region, a new boundary integral equation, proposed by the authors for multi-layered elasto-static axisymmetric medium, is used. With the new boundary integral equation, only the top surface in contact area is needed to be discretized into elements and the re-mesh during the optimization may be avoided. For convenience of symbolism, the homogeneous region is denoted as domain A and the multi-layered region is denoted as domain B.

At first, the boundary element method for domain A is investigated. By using the ordinary boundary integral equation, discretizing the elements and approximating the boundary data over each element by a set of interpolating function, the boundary element equations for domain A are obtained as

$$\sum_{j=1}^{N_t} \boldsymbol{H}_{ij}^A \boldsymbol{u}_j^A + \sum_{j=1}^{N_q} \boldsymbol{H}_{ij}^A \boldsymbol{u}_j^A + \sum_{j=1}^{N_c} \boldsymbol{H}_{ij}^A \boldsymbol{u}_j^A = \sum_{j=1}^{N_t} \boldsymbol{G}_{ij}^A \boldsymbol{q}_j^A + \sum_{j=1}^{N_q} \boldsymbol{G}_{ij}^A \boldsymbol{q}_j^A + \sum_{j=1}^{N_c} \boldsymbol{G}_{ij}^A \boldsymbol{q}_j^A, \quad i = 1, 2, \ldots, N_t + N_q + N_c, \tag{1}$$

where N_t, N_q and N_c are the number of nodes in the part prescribed by traction, the part prescribed by displacement and the contact part of the boundary, respectively. The vectors, $\boldsymbol{u}_j^A$ and $\boldsymbol{q}_j^A$, are the displacement vector and the traction vector at node j.

For the domain B, the multi-layered region, by using the Hankel's transforms and the system matrix approach, the relationships between the stresses and displacement on the top surface and those on the bottom surface are given by Wang and Ishikawa (1999, 2000) as

$$\overline{\mathbf{a}}_N(h_N) = \mathbf{T}_N(h_N)\overline{\mathbf{a}}_1(0) \tag{2}$$

and

$$\overline{\mathbf{b}}_N(h_N) = \overline{\mathbf{B}}_N\overline{\mathbf{a}}_N(h_N), \tag{3}$$

where the subscript 1 means the bottom layer and the subscript N means the top layer, matrices, $\mathbf{T}_N(h_N)$ and $\overline{\mathbf{B}}_N$ (see Appendix A) are the transferring matrix and

$$\overline{\mathbf{a}}_N(h_N) = (H_0\sigma_{zz}(h_N), H_1\sigma_{zr}(h_N), H_1u_r(h_N), H_0u_z(h_N))^{\mathrm{T}},$$
$$\overline{\mathbf{b}}_N(h_N) = (H_2(\sigma_{rr}(h_N) + \sigma_{\theta\theta}(h_N)), H_0(\sigma_{rr}(h_N) - \sigma_{\theta\theta}(h_N)))^{\mathrm{T}},$$

whereby H_n $(n = 1, 2, \ldots)$ is Hankel's transform defined as

$$\bar{f}^{(n)}(\alpha) = H_n\{f(r)\} = \int_0^\infty rf(r)I_n(\alpha r)\,\mathrm{d}r,$$

where α is a variable and $n = 0, 1, 2, \ldots$.

After applying the inverse Hankel's transform defined as

$$f(r) = H_n^{-1}\{f^{(n)}(\alpha)\} = \int_0^\infty \alpha f^{(n)}(\alpha)I_n(\alpha r)\,\mathrm{d}\alpha$$

to Eqs. (2) and (3), a relationship between the displacement and stresses on the top surface can be obtained as

$$\begin{pmatrix} u_r(h_N) \\ u_z(h_N) \end{pmatrix} = f(H_0\sigma_{zz}(h_N), H_1\sigma_{zr}(h_N))$$

(Wang and Ishikawa, 2000). The right-hand side of the relationship is a vector, the elements of which are integrals with a semi-infinite interval. Since the stresses on the top surface exist only on the contact area, the elements are discretized only in the contact area of the top surface of domain B. Finally, the system equation for the domain B is given as

$$\boldsymbol{u}_i^B = \sum_{j=1}^{N_c} \boldsymbol{H}_{ij}^B\boldsymbol{q}_j^B, \quad i = 1, 2, \ldots, N_c, \tag{4}$$

where N_c is just the same as that described in Eq. (1).

In the present study, it is assumed that there is no friction happened during the contact. Thus the contact conditions can be described as

$$q_n^a = q_n^b, \tag{5}$$

$$q_t^a = q_t^b = 0, \tag{6}$$

$$u_n^a - u_n^b = \Delta u_n^{ab}, \tag{7}$$

where a and b denote a contact node pair, which are belonged to domains A and B, respectively, n means normal direction, t means tangential direction and Δu_n^{ab} is the gap between the two candidate contact nodes a and b.

Subsequently, the contact problem between a homogeneous body and a multi-layered medium can be solved by the presented boundary element Eqs. (1) and (4) with contact conditions (5)–(7).

3. Optimization process

The estimation of material properties for the present inverse problem may be viewed as optimization approach. Let $\mathbf{u}^* = (u_1^*, u_2^*, \ldots, u_M^*)$ be the measured or specified displacements and $\tilde{\mathbf{u}} = (\tilde{u}_1, \tilde{u}_2, \ldots, \tilde{u}_M)$ be the calculated displacements, where the subscripts 1, 2, ..., M may mean the different measured or specified locations in the domains under consideration, or it may mean the load steps. The unknown material properties are defined in a vector as $\mathbf{p} = (E_1, h_1, E_2, h_2, \ldots)^{\mathrm{T}}$. There will be a relationship $\tilde{\mathbf{u}} = f(\mathbf{p})$ between $\tilde{\mathbf{u}}$ and $\mathbf{p}$ when boundary element method is employed. Obviously, the relationship behaves nonlinearly.

3.1. The objective function

Our goal is to seek an approach to minimize the error between $\mathbf{u}^*$ and $\tilde{\mathbf{u}}$, and it may be expressed in mathematical notation as follows:

$$\min \|\mathbf{u}^* - \tilde{\mathbf{u}}\|. \tag{8}$$

The measuring of the error is considered in the Euclidean space in the present work, and the objective function to be minimized is written as a least squares as:

$$\Phi(\mathbf{p}) = \tfrac{1}{2}\left(\mathbf{u}^* - \tilde{\mathbf{u}}\right)\left(\mathbf{u}^* - \tilde{\mathbf{u}}\right)^{\mathrm{T}}. \tag{9}$$

3.2. Constraints

In order to keep a physical meaning during optimization, some constraint conditions must be applied to the minimization procedure. Based on the physics of this problem, the constraints are expressed as

$$c_j(\mathbf{p}) \geqslant 0, \ j = 1, \ldots, L, \tag{10}$$

where L is the number of constrains and c_j are the constrain functions. The choice of the constraints will be discussed later during the numerical analysis. The set of $\mathbf{p}$ that satisfies the constraints is called the feasible region. It is important to maintain the feasibility of the parameters throughout the optimization process. In order to obtain a reasonable determination, predicted conditions, such as predicted bounds of Young's modulus and the predicted geometrical shapes can be considered as constraints. Constrained minimization problems cannot be solved directly. They must be transformed into unconstrained problems. The frequently used methods to transform a constrained problem to an unconstrained one are the change of variables, internal penalty function and external penalty function. The change of variables can result in eccentricity in the objective function (9) and make the convergence more difficult. The external penalty function approaches to the minimum value from outside, i.e. from the point located in the infeasible region. Obviously, this method cannot be employed to solve this problem. Hence, internal penalty function is adopted in the present study. The constraints are incorporated directly in the objective function $\Phi^*(\mathbf{p})$ given as

$$\Phi^*(\mathbf{p}) = \Phi(\mathbf{p}) + \sum_{j=1}^{q} \zeta_j(\mathbf{p}), \tag{11}$$

where the weighted penalty function, ζ_j, is the inverse barrier function proposed by Carroll (1961) as

$$\zeta_j(\mathbf{p}) = w_j / c_j(\mathbf{p}), \tag{12}$$

whereby w_j is nonnegative weights.

3.3. A modified Levenberg–Marquardt's method

Starting from an initial feasible guess of parameter $\mathbf{p}$, the modified Levenberg–Marquardt's method (Ravi and Jennings, 1990) employs a sequence of corrections to the parameter until the convergence is achieved, according to some specified criteria. The parameter correction, $\Delta\mathbf{p}$, at iteration k is calculated from the following system of equations as

$$\left(\mathbf{J}^{(k)T}\mathbf{J}^{(k)} + \Lambda^{(k)}\mathbf{I} + \mathbf{H}^{(k)}\right)\Delta\mathbf{p}^{(k)} = -\mathbf{J}^{(k)\mathrm{T}}\left(\tilde{\mathbf{u}} - \mathbf{u}^*\right)^{(k)} + \mathbf{g}^{(k)}, \tag{13}$$

where Λ is the Levenberg–Marquardt parameter, a nonnegative scalar. $\mathbf{J}$ is the Jacobian matrix of $\Phi(\mathbf{p})$, and $\mathbf{I}$ is the identity. Let set $r_i = \tilde{u}_i - u_i^*$. The elements of $\mathbf{J}$, $\mathbf{g}$ and $\mathbf{H}$ are given by

$$J_{i\alpha} = \partial r_i / \partial p_\alpha = \partial \tilde{u}_i / \partial p_\alpha, \quad i = 1, M, \ \ \alpha = 1, \ldots, n, \tag{14}$$

$$g_\alpha = -\sum_{j=1}^{q} \partial \zeta_j / \partial p_\alpha, \quad \alpha = 1, \ldots, n, \tag{15}$$

$$H_{\alpha\beta} = \sum_{j=1}^{q} \partial^2 \zeta_j / \partial p_\alpha \partial p_\beta, \quad \alpha, \beta = 1, \ldots, n, \tag{16}$$

where n is the number of the elements of parameter $\mathbf{p}$. If linear constraints are employed, the first and the second derivatives of the penalty functions, which are used in expressions (15) and (16), can be expressed as

$$\partial \zeta_j / \partial p_\alpha = -(w_j / c_j^2) \partial c_j / \partial p_\alpha, \quad j = 1, \ldots, L, \ \ \alpha = 1, \ldots, n, \tag{17}$$

$$\partial^2 \zeta_j / \partial p_\alpha \partial p_\beta = (2 w_j / c_j^3)(\partial c_j / \partial p_\alpha)(\partial c_j / \partial p_\beta), \quad j = 1, \ldots, L, \ \ \alpha, \beta = 1, \ldots, n. \tag{18}$$

Marquardt (1963) proved that as the Levenberg–Marquardt parameter, Λ, which determines the direction and the size of the parameter step, $\Delta\mathbf{p}$, tends to infinity, the direction of the step rotates toward the steepest descent direction and the step size tends to zero. Therefore, a sufficiently large, positive value should be prescribed to Λ in order to ensure that the step is taken in a descent direction, i.e. $\Phi^*(\mathbf{p})^{(k+1)} < \Phi^*(\mathbf{p})^{(k)}$.

Although we have the definition of Jacobian matrix $\mathbf{J}$ as described in expression (14), we cannot compute it directly. In the present study, a finite difference approximation of $\mathbf{J}$ is used by the present boundary element with perturbing the parameter at each iteration.

3.4. Solution algorithm

Similarly to the algorithm for the determination of an elastic inclusion in a finite matrix using the finite element method, which is presented by Schnur and Zabaras (1992), an optimization algorithm that combines the present boundary element method and the modified Levenberg–Marquardt's method is designed to determine the elastic properties or thickness of the specified layers. The detailed algorithm is given as follows:

1. Guess an initial value to the parameter, $\mathbf{p}^{(0)}$, and the Levenberg–Marquardt parameters (Marquardt, 1963), $\Lambda^{(0)} = 0.01$.

2. Generate boundary element mesh, solve the boundary element contact problem at $\mathbf{p}^{(0)}$ for the displacement, $\tilde{\mathbf{u}}^{(0)}$, at the measurement locations and evaluate the error function, $\Phi^{(0)}$.
3. Set the initial penalty function weights (Ravi and Jennings, 1990), $w_j^{(0)} = 0.001 c_j^{(0)} \Phi^{(0)}$, $j = 1, L$. Evaluate the weighted penalty function, $\zeta_j^{(0)}$, $j = 1, L$, and objective function, $\Phi^{*(0)}$.
4. Begin the kth iteration loop

(A) Calculate Jacobian Matrix, $\mathbf{J}^{(k)}$, by the finite difference approximation with the displacement increment, Δu, which is obtained by the boundary element method with perturbation the parameter $\mathbf{p}^{(k)}$.
(B) Calculate the penalty function derivatives to form $\boldsymbol{H}^{(k)}$ and $\boldsymbol{g}^{(k)}$ using Eqs. (17) and (18).
(C) Solve Eq. (13) for the parameter increment, $\Delta\mathbf{p}^{(k)}$, and update the parameter, $\mathbf{p}^{(k+1)} = \mathbf{p}^{(k)} + \Delta\mathbf{p}^{(k)}$.
(D) Solving the contact problem using boundary element method with the new obtained material parameters $\mathbf{p}^{(k+1)}$.
(E) Evaluate $\zeta_j^{(k+1)}$, $j = 1, L$, and objective function, $\Phi^{*(k+1)}$.
(F) Check if $\Phi^{*(k+1)} < \Phi^{*(k)}$. If false, increase Λ and go to 4(C); If true, continue.
(G) Decrease w_j and Λ.
(H) Check if iteration has converged with criteria (10) $|\delta_i^k|/(\gamma + |p_i^k|) < \varepsilon$ ($i = l,\ n$, and small $\varepsilon, \gamma > 0$). If false, set $k = k + 1$ and go to 4(A); If true, stop, the properties are determined as $\mathbf{p}^{(k)}$.

4. Numerical Studies

To test the above-mentioned method, two ideal models about the multi-layered medium indented by the homogeneous indenters are investigated with the algorithm described in Section 3. The measured or specified displacements, or the elements of the vector, $\tilde{\mathbf{u}}$, may be the displacements at different location in the investigated domain produced by the one indenter, or may be the displacement at the same location in the investigated domain produced by the different indenters. The latter case needs much long time due to element re-mesh. Therefore, without losing the generality, the former case is chosen in the present numerical test.

4.1. Model A

This model is about a two-layer medium indented by sphere indenter (Fig. 2). The two-layered medium is placed on a rigid foundation, and this means its bottom surface is simply supported in the view of the mechanics. The top layer is very thinner than that of the bottom layer. The specified displacement is taken at a set of points on the top surface of the two-layer medium. The element discretization used in the present boundary element method is shown in Fig. 3. In order to ensure the accuracy of the computation, the sphere boundary is divided into 40 quadratic elements, and the candidate contact area and the area

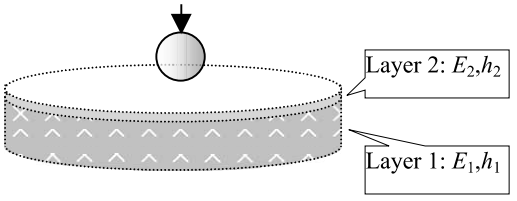

Fig. 2. A two-layer medium indented by a sphere body.

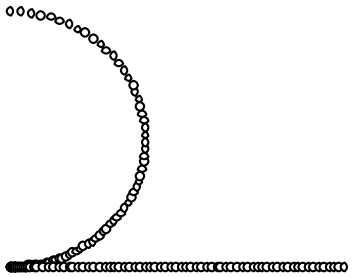

Fig. 3. The boundary element model for analyzing the problem of model A.

including specified points are meshed into 40 quadratic elements only in the present boundary element method for analyzing the model. The radius of the cross of the sphere indenter is $r = 2.0$ μm and its Young's modulus is 1000 GPa. The parameters to be determined may be Young's modulus and the thickness of the two layers. Two cases are investigated as follows:

The first case: Young's modulus of the two layers are known, and $\mathbf{p} = (h_1, h_2)$,

The second case: all the parameters of the two layers are unknown, and $\mathbf{p} = (h_1, E_1, h_2, E_2)$.

The true value of the parameter is $\mathbf{p}$ = (206 GPa, 9.2 μm, 150 GPa, 0.2 μm). To ensure the uniqueness of the solution, 10 constraints are designed as:

$$c_1 = E_1 \geqslant 0 \quad c_2 = E_1^{\max} - E_1 \geqslant 0,$$

$$c_3 = E_2 \geqslant 0 \quad c_4 = E_2^{\max} - E_2 \geqslant 0,$$

$$c_5 = h_1 \geqslant 0 \quad c_6 = h_1^{\max} - h_1 \geqslant 0,$$

$$c_7 = h_2 \geqslant 0 \quad c_8 = h_2^{\max} - h_2 \geqslant 0,$$

$$c_9 = h_1 - h_2 \geqslant 0 \quad c_{10} = h - h_1 - h_2 \geqslant 0,$$

where $E_1^{\max} = E_2^{\max} = 300$ GPa, $h = h_1^{\max} = 9.4$ μm and $h_2^{\max} = 2.0$ μm. All of the above constraints are linear constraints. Constraints, c_1, c_3, c_5, c_7, keep Young's modulus and the thickness always positive, constraints, c_2, c_4, c_6, c_8, force Young's modulus and the thickness to be in some limited ranges. For the first case, constraints, c_5, c_6, c_7, c_8, c_9 and c_{10}, are employed. As for the second case, all constraints are valid in analysis. In all cases, the load condition is to prescribe a displacement, 0.01 μm, to the top point of the sphere, and the convergence criterion are $\gamma = \varepsilon = 1.0 \times 10^{-4}$. The model is first analyzed by the conventional boundary element method with the true parameter $\mathbf{p}$ = (206 GPa, 9.2 μm, 150 GPa, 0.2 μm). The distribution of the normal displacement on the top surface of the two-layer medium is shown in Fig. 4, and a large view of that distribution in the neighborhood of the axis is depicted in Fig. 5.

Totally 20 points are specified and they locate on the top surface of the two-layer medium. Their radial coordinates and normal displacements, which are the elements of the vector $\mathbf{u}^* = (u_1^*, u_2^*, \ldots, u_{20}^*)$, are given in Table 1.

During the optimizing procedure, the displacements at the specified points, which are the elements of the vector, $\tilde{\mathbf{u}} = (\tilde{u}_1, \tilde{u}_2, \ldots, \tilde{u}_M)$, are computed by the present boundary element method. Different initial parameters are tested. The ideal results are described as the following:

The first case: the final initial values prescribed to the parameter are $\mathbf{p}^{(0)}$ = (250 GPa, 9.2 μm, 250 GPa, 0.2 μm).

The perturbing value of the parameter, or the interval, used by the finite difference in calculating the Jacobian matrix, $\mathbf{J}$, is given as

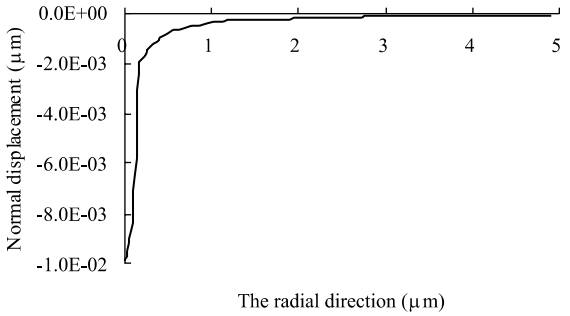

Fig. 4. The distribution of displacement on the top surface of the two-layer medium.

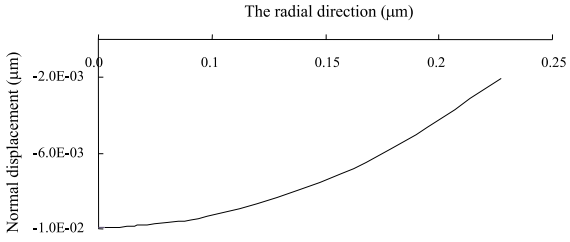

Fig. 5. A large view of Fig. 4 in the neighborhood of $R = 0$.

Table 1
The radial coordinates (μm) and normal displacements (μm) of the specified points

R coordinate	Displacement	R coordinate	Displacement
2.91E − 03	−9.9213192E − 03	2.04E − 01	−1.8212214E − 03
1.26E − 02	−9.8837104E − 03	2.34E − 01	−1.7263844E − 03
3.01E − 02	−9.6975423E − 03	2.64E − 01	−1.5409463E − 03
4.07E − 02	−9.5087773E − 03	3.31E − 01	−1.2157446E − 03
6.98E − 02	−8.7046897E − 03	3.69E − 01	−1.0867756E − 03
8.82E − 02	−7.9763582E − 03	4.07E − 01	−9.8294725E − 04
1.07E − 01	−7.0779877E − 03	5.57E − 01	−7.0829002E − 04
1.29E − 01	−5.7627623E − 03	6.32E − 01	−6.1933463E − 04
1.51E − 01	−4.1978101E − 03	7.83E − 01	−4.9170901E − 04
1.77E − 01	−2.0415078E − 03	9.34E − 01	−4.0454777E − 04

$$\Delta\mathbf{p} = (\Delta h_1, \Delta h_2) = (1.0 \times 10^{-4}\ \mu\text{m}, 1.0 \times 10^{-4}\ \mu\text{m}).$$

The obtained parameters when the convergence is achieved are given in Table 2.

The second case: The initial values prescribed to the parameter are $\mathbf{p}^{(0)} = (h_1, E_1, h_1, E_2) = (9.0\ \mu\text{m}, 250\ \text{GPa}, 250\ \text{GPa}, 0.4\ \mu\text{m})$.

The perturbing value of the parameter, or the interval, used by the finite difference in calculating the Jacobian matrix, **J**, is given as

$$\Delta\mathbf{p} = (\Delta h_1, \Delta E_1, \Delta h_1, \Delta E_2) = (1.0 \times 10^{-4}\ \mu\text{m},\ 0.5\ \text{GPa},\ 1.0 \times 10^{-4}\ \mu\text{m},\ 0.5\ \text{GPa}).$$

The obtained parameters when the convergence is achieved are given in Table 3.

Table 2
The estimated parameters for the first case

Status	Parameters	
	h_1 (μm)	h_2 (μm)
True	9.2	0.2
Initial	9.0	0.4
Estimated	9.20139	0.1986

Table 3
The estimated parameters for the second case

Status	Parameters			
	h_1 (μm)	E_1 (GPa)	h_2 (μm)	E_2 (GPa)
True	9.2	206.0	0.2	150.0
Initial	9.0	250.0	0.4	250.0
Estimated	9.20252	209.732	0.19751	153.319

It can be found in the second case that the accuracy of the estimated thickness is higher than that of Young's modulus. The phenomenon is due to that the more constraints are prescribed to the thickness parameters. It is found that the choice of the initial parameters is fundamental importance in the present model. If the initial parameters deviate too far from the true parameters, the estimated parameters are eccentric.

4.2. Model B

This model is about a four-layer medium indented by a cylindric indenter (Fig. 6). Analogously to the conditions described in the Section 4.1, the four-layered medium is placed on a rigid foundation, and that means that the bottom surface of the medium is simply supported in the view of the mechanics. The top three layers are very much thinner than that of the bottom layer. The specified displacements take at a set of points on the top surface of the layered medium. The element discretization used in the present boundary element method is shown in Fig. 7. The radius of the cross-section of the cylindrical punch is $r = 1.0$ μm and its Young's modulus is 1000 GPa. The parameters to be determined are

$$\mathbf{p} = (h_1, E_1, h_2, E_2, h_3, E_3, h_4, E_4).$$

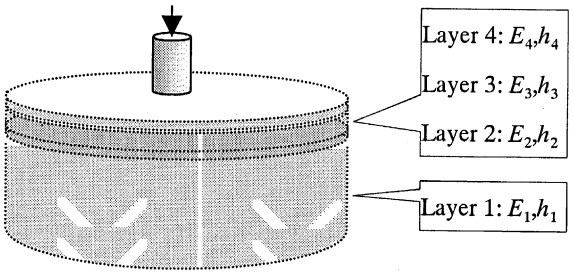

Fig. 6. A four-layer medium indented by a cylindrical body.

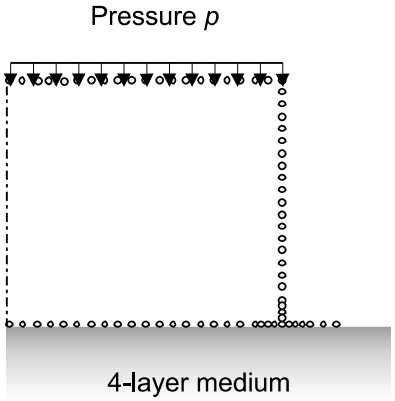

Fig. 7. Quadratic element discretization used for model B.

The true value of the parameters is

$$\mathbf{p} = (9.2\ \mu\text{m}, 206\ \text{GPa}, 0.2\ \mu\text{m}, 250\ \text{GPa}, 0.2\ \mu\text{m}, 200\ \text{GPa}, 0.2\ \mu\text{m}, 150\ \text{GPa}).$$

Twenty constraints are given in the following table as:

$c_1 = E_1 \geqslant 0$	$c_5 = E_3 \geqslant 0$
$c_2 = E_1^{\max} - E_1 \geqslant 0$	$c_6 = E_3^{\max} - E_3 \geqslant 0$
$c_3 = E_2 \geqslant 0$	$c_7 = E_4 \geqslant 0$
$c_4 = E_2^{\max} - E_2 \geqslant 0$	$c_8 = E_4^{\max} - E_4 \geqslant 0$
$c_9 = h_1 \geqslant 0$	$c_{15} = h_3^{\max} - h_3 \geqslant 0$
$c_{10} = h_1^{\max} - h_1 \geqslant 0$	$c_{16} = h_1 - h_3 \geqslant 0$
$c_{11} = h_2 \geqslant 0$	$c_{17} = h_4 \geqslant 0$
$c_{12} = h_2^{\max} - h_2 \geqslant 0$	$c_{18} = h_4^{\max} - h_4 \geqslant 0$
$c_{13} = h_1 - h_2 \geqslant 0$	$c_{19} = h_1 - h_4 \geqslant 0$
$c_{14} = h_3 \geqslant 0$	$c_{20} = h - h_1 - h_2 - h_3 - h_4 \geqslant 0$

where

$$E_1^{\max} = E_2^{\max} = E_3^{\max} = E_4^{\max} = 300\ \text{GPa}, h = h_1^{\max} = 9.4\ \mu\text{m},$$

and $h_2^{\max} = h_3^{\max} = h_4^{\max} = 0.4\ \mu\text{m}$. It is obvious that all of the above constraints are linear constraints. The load condition is to prescribe a pressure, $p = 1$ mN, to the top of the cylindrical punch, and the convergence criterion are $\gamma = \varepsilon = 1.0 \times 10^{-4}$. Similarly to the procedure in Section 4.1, the model is first analyzed by the conventional boundary element method with the true parameter. Totally 14 points are specified and they locate on the top surface of the four-layer medium. Their radial coordinates and normal displacements, which are the elements of the vector $\mathbf{u}^* = (u_1^*, u_2^*, \ldots, u_{14}^*)$, are given in Table 4.

The perturbing value of the parameter $\mathbf{p}$ is the same as the one given in the model A.

A set of ideal result, which are optimized the presented algorithm with numerical tests, is given in Table 5.

The accuracy of the estimated Young's modulus is not better than that of the thickness and it can be improved by giving more constraints to Young's modulus.

Table 4
The radial coordinates (μm) and normal displacements (μm) of the specified points

R coordinate	Displacement	R coordinate	Displacement
0.00	7.5108915E − 03	0.35	7.4550417E − 03
0.05	7.5097694E − 03	0.40	7.4376211E − 03
0.10	7.5063930E − 03	0.45	7.4176381E − 03
0.15	7.5007440E − 03	0.50	7.3950121E − 03
0.20	7.4928233E − 03	0.55	7.3695458E − 03
0.25	7.4825864E − 03	0.60	7.3410917E − 03
0.30	7.4700163E − 03	0.65	7.3092886E − 03

Table 5
The estimated parameters for the second case

Status	Parameters							
	h_1 (μm)	E_1 (GPa)	h_2 (μm)	E_2 (GPa)	h_3 (μm)	E_3 (GPa)	h_4 (μm)	E_4 (GPa)
True	9.2	206.0	0.2	250.0	0.4	200.0	0.2	150.0
Initial	9.0	250.0	0.33	250.0	0.33	250.0	0.33	200.4
Estimated	9.20311	210.732	0.19842	248.319	0.38904	207.570	0.20943	155.277

5. Discussion and conclusions

An algorithm to solve the inverse problems about the estimation of material properties of the multi-layered media was developed. The present method combines a particular boundary element method and a modified Levenberg–Marqardt method. The estimation of the parameters of two ideal models was investigated. Although the algorithm is easy, the estimated results may be conquered by many factors, such as the constraints, the initial value prescribed to the parameters, or the error of the data and so on, because the inverse problem is ill posed. The estimated parameters of two investigated ideal models are obtained with many constraints and the values of the initial parameters in the neighborhood of the true parameters. Eccentric results were produced when the constraints were few or the initial parameters were far from the true ones. The more parameters are considered, the more difficulty is yield to guarantee the uniqueness of the solution. The effect of the data error was discussed by Schnur and Zabaras (1992). The present method is efficient and may be applied to solve some indentation problems, if a good pro-estimation is made in advance.

Acknowledgements

The authors wish to express their thanks to Professor Xing Ji of Tongji University, China, for his useful advice.

Appendix A

The matrix $\mathbf{T}_N(h_N)$ was obtained as

$$\mathbf{T}_N(h_N) = \mathbf{X}_N(h_N)\mathbf{X}_N^{-1}(h_{N-1})\mathbf{X}_{N-1}(h_{N-1})\cdots\mathbf{X}_2^{-1}(h_1)\mathbf{X}_1(h_1)\mathbf{X}_1^{-1}(0), \tag{A.1}$$

where the matrix $\mathbf{X}_k(z)$ is

$$\begin{pmatrix} d_k \sinh(\alpha z) & d_k \cosh(\alpha z) & c_k \cosh(\alpha z) - 2\alpha c_k z \sinh(\alpha z) & c_k \sinh(\alpha z) - 2\alpha c_k z \cosh(\alpha z) \\ -d_k \cosh(\alpha z) & -d_k \sinh(\alpha z) & c_k \sinh(\alpha z) + 2\alpha c_k z \cosh(\alpha z) & c_k \cosh(\alpha z) + 2\alpha c_k z \sinh(\alpha z) \\ -\sinh(\alpha z) & -\cosh(\alpha z) & \cosh(\alpha z) + \frac{2\alpha c z \sinh(\alpha z)}{d} & \sinh(\alpha z) + \frac{2\alpha c_k z \cosh(\alpha z)}{d_k} \\ \cosh(\alpha z) & \sinh(\alpha z) & \sinh(\alpha z) - \frac{2\alpha c_k z \cosh(\alpha z)}{d_k} & \cosh(\alpha z) - \frac{2\alpha c_k z \sinh(\alpha z)}{d_k} \end{pmatrix} \tag{A.2}$$

and

$$c_k = \frac{E_k \alpha}{(1+v_k)(3-4v_k)}, \quad d_k = \frac{E_k \alpha}{1+v_k}, \quad k = 1, 2, 3, \ldots, N.$$

The matrix $\bar{\mathbf{B}}_k$ was obtained as

$$\bar{\mathbf{B}}_k = \begin{pmatrix} \frac{2v_k}{1-v_k} & 0 & \frac{E_k}{1-v_k}\alpha_k & 0 \\ 0 & 0 & -\frac{E_k}{1+v_k}\alpha_k & 0 \end{pmatrix}. \tag{A.3}$$

References

Becker, A.A., 1992. The Boundary Element Method in Engineering. McGraw-Hill, New York.

Bhattacharya, A.K., Nix, W.D., 1988. Analysis of elastic and plastic deformation associated with indentation test of thin films on substrates. Int. J. Solids Struct. 24, 1287–1298.

Carroll, C.W., 1961. The created response surface technique for optimizing nonlinear restrained systems. Oper. Res. 9, 169–184.

Chiang, T.L., Dulikravich, G.S., 1986. Inverse design of composite turbine blade circular coolant flow passages. J. Turbomachinery ASME 108, 275–282.

Doerner, M.F., Nix, W.D., 1986. A method for interpretating the data from depth-sensing indentation instruments. J. Mater. Res. 1 (4), 601–609.

Gao, H., Chiu, C., Lee, J., 1992. Elastic contact versus indentation modeling of multi-layered materials. Int. J. Solids Struct. 29, 2471–2492.

King, R.B., 1987. Elastic analysis of some punch problems for a layered medium. Int. J. Solids Struct. 23, 1657–1664.

Laursen, T.A., Simo, J.C., 1992. A study of the mechanics of microindentation using finite elements. J. Mater. Res. 7, 618–626.

Loubet, J.L., Georges, J.M., Marchesini, O., Meille, G., 1984. Vickers indentation curves of magnesium oxide (MgO). J. Tribology 106, 43–48.

Marquardt, D.W., 1963. An algorithm for least squares estimation of nonlinear parameters. J. Soc. Indust. Appl. Math. 11, 431–440.

Menick, J., Munz, D., Quandt, E., Ludwig, A., 1999. Determination of elastic modulus of thin layers. Z. Metallkd 90, 766–773.

Ravi, V., Jennings, A.A., 1990. Penetration model parameter estimation for dynamic permeability measurements. Soil Sci. Soc. Am. J. 54, 13–19.

Schnur, D.S., Zabaras, N., 1992. An inverse method for determining elastic material properties and a material interface. Int. J. Numer. Meth. Engng. 33, 2039–2057.

Shield, T.W., Body, D.B., 1989. Some axisymmetric problems for layered elatsic media: part I – multiple region contact solutions for simply-connected indenters. J. Appl. Mech. 56, 798–806.

Swain, M.V., 1998. Mechanical properties characterisation of small volumes of brittle materials with spherical tipped indenters. Mater. Sci. Engng. A – Struct. 253, 160–166.

Tanaka, M., Yamagiwa, K., 1989. A boundary element method for some inverse problems in elastodynamics. Appl. Math. Modelling 13, 307–312.

Trujillo, D.M., 1997. In: Busby, H.R. (Ed.), Practical Inverse Analysis in Engineering. CRC press, New York.

Tsui, T.Y., Pharr, G.M., 1999. Substrate effects on nanoindentation mechanical property measurement of soft films on hard substrates. J. Mater. Res. 14, 292–301.

Wang, W., Ishikawa, H., 1999. A fundamental solution for the axisymmetric elastostatic single layered medium. Proceedings of the Sixteenth Japan National Symposium on Boundary Element Methods. Tokyo, pp. 25–30.

Wang, W., Ishikawa, H., 2000. A method for linear elasto-static multi-layered axisymmetrical problems using Hankel's transform. Computat. Mech., accepted for publication.

Yu, H.Y., Sanday, S.C., Rath, B.B., 1990. The effect of substrate on the elastic properties of films determined by the indentation test – axisymmetric Bousinesq problem. J. Mech. Phys. Solids 38, 745–764.

Zabaras, N., Morellas, V., Schnur, D., 1989. A spatially regularized solution of inverse elasticity problems using the boundary element methods. Commun. Appl. Numer. Meth. 5, 547–553.